UNIVERSITY
OF
QUEENSLAND

Department of Civil Engineering

RESEARCH REPORT SERIES

Inelastic Beam Buckling Experiments

P. F. DUX and
S. KITIPORNCHAI

Research Report No. CE24
May, 1981

CIVIL ENGINEERING RESEARCH REPORTS

This report is one of a continuing series of Research Reports published by the Department of Civil Engineering at the University of Queensland. This Department also publishes a continuing series of Bulletins. Lists of recently published titles in both of these series are provided inside the back cover of this report. Requests for copies of any of these documents should be addressed to the Departmental Secretary.

Department of Civil Engineering,
University of Queensland,
St Lucia, Q 4067, Australia,
[Tel:(07) 377-3342, Telex:UNIVQLD AA40315]

INELASTIC BEAM BUCKLING EXPERIMENTS

by

P. F. Dux, BE, M Eng Sc.
Senior Tutor in Civil Engineering

and

S. Kitipornchai, BE, PhD
Senior Lecturer in Civil Engineering

RESEARCH REPORT NO. CE 24
Department of Civil Engineering
University of Queensland
May, 1981

Synopsis

This report describes a series of experiments on the buckling of simply supported laterally continuous I-beams in the inelastic range. Nine beams were tested in three groups of three, each group having a different predominant moment gradient. Points of load application were prevented from moving laterally and twisting. Measurements of geometrical and material imperfections are included in the report. Results of a number of subsidiary experiments such as plastic moment and stub column tests are also presented.

The results add to the small amount of test data presently available on such beams and provide a comparison with theoretical predictions. In particular, support is shown for the theoretical curves of Nethercot and Trahair and for the current trend to multiple design curves based on moment gradient.

CONTENTS

Don 1981 Fryer

1. INTRODUCTION

A study of the literature shows that there are several analytical methods of predicting the elastic and inelastic buckling loads of I-beams with various imperfections and loading and support arrangements. Differences between the methods are found in the numerical analysis techniques adopted and , particularly with inelastic buckling analyses, in the sophistication of the theoretical models. Extensive testing has demonstrated the accuracy of elastic buckling solutions and the soundness of the underlying theory. This is evident in many references (e.g. 1, 2, 3) where consistent analytical and experimental results are presented for a wide range of beams. The Australian code (4) expressly permits the use of elastic buckling analysis as an alternative to the code formula. By comparison, the theory and solutions for inelastic beam buckling have not been as widely verified and current design rules for inelastic beams (4, 5, 6) are less liberal. Some of the factors responsible for this are discussed briefly in the following paragraphs.

Because inelastic behaviour is influenced by material and geometrical imperfections, experiments need to be full scale. The high resource implications have resulted in relatively few tests being conducted. Fukumoto and Kubo (7) have identified 95 inelastic rolled beam experiments, most of which involved uniform determinate beams carrying either two point loads producing a uniform major axis moment or an unbraced central point load. While the emphasis on severe loading was necessary a consequence is that test results are not available for other common loading configurations. For example, little information is available on beams with braced loads producing general moment gradients.

Verification of inelastic buckling theory is made more difficult by the manner in which some programs of experiments have been conducted and reported. Sometimes information on residual stresses or geometrical imperfections is omitted. Kitipornchai and Trahair (8) comment on the non-uniformity of loading rates which has helped to accentuate scatter between the results of different testing programs. Also, the quality of apparatus varies. Dibley (9) estimates significant frictional effects in one third of his experiments.

In the absence of test results, some researchers have used theoretical solutions to develop new design methods and design rules. In particular, this has been done for simply supported beams with unequal major axis end moments (12, 13, 14) and for determinate laterally continuous beams with braced load points (12). Theory predicts that segment continuity coupled with more favourable segment moment gradients can result in capacities well in excess of those implied by code formulae based on tests with the more severe loadings. Other researchers (15, 16) while aware of these likely benefits have taken the cautious approach of recommending new design rules based on experimental data alone. There is little doubt that the more radical proposals require experimental backing if they are to receive the wide acceptance they probably deserve. Galambos (10) outlines the need for further careful testing. He expects that current inelastic buckling theory will be confirmed, presumably by closer agreement than that demonstrated in Ref. 8, by Vinnakota (11) and by others.

The immediate aim of the experiments described herein was to study the variation of inelastic beam capacity with changing moment gradient. The test results and measurements would add also to the data available for use by other researchers.

2. PLANNING FOR EXPERIMENTS

2.1 Test Beam Moment Gradients

Figure 1 shows the theoretical capacity curves for simply supported beams under end moments (12) which have been used in Refs. 12-14 as the basis for new design aids. High levels of flange tip compressive residual stress have been adopted in an effort to account for geometrical as well as material imperfections. Included in the figure is a cross-hatched region containing most of the test results reported in the open literature and summarised in references such as Refs. 7 and 15. The limited range is clearly illustrated.

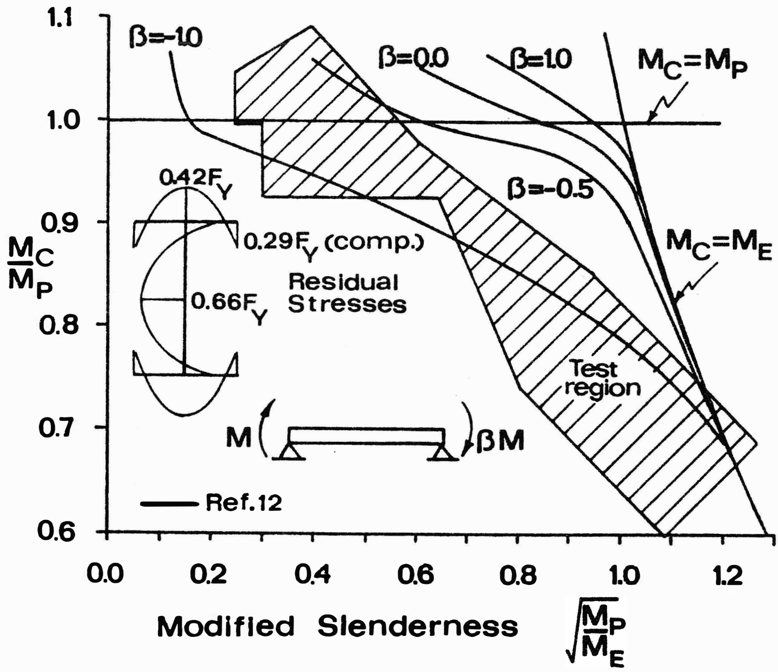

FIGURE 1: Capacity curves for moment gradient beams.

Marked changes occur in the theoretical curves across the moment gradient range $-1.0 < \beta < 0.0$ where the gradient, β, is the ratio of end moments and equals -1.0 for uniform bending. The capacity curves of beams with higher gradients ($\beta > 0.0$ follow the elastic buckling line closely until the plastic moment is approached. It was decided to use the resources available to test beams in the lower moment gradient range. Three gradient were selected - to the extremes of $\beta = -1.0$ and $\beta = 0.0$ was added $\beta = -0.7$ which was estimated to provide something of a median capacity curve. The uniform moment load case was chosen as it was felt that a series of tests with newly devised apparatus ought to include the most severe loading. A total of nine beams was tested in three groups of three, each group having one of the moment gradients.

2.2 Loading Configurations

The loading arrangements are shown in Fig. 2. The figure lists the test beam lengths and gives the order in which the experiments were conducted. Beam cross-sections at each load and support point were prevented from moving laterally and from twisting. The devices used to achieve this simple bracing are discussed in a later section.

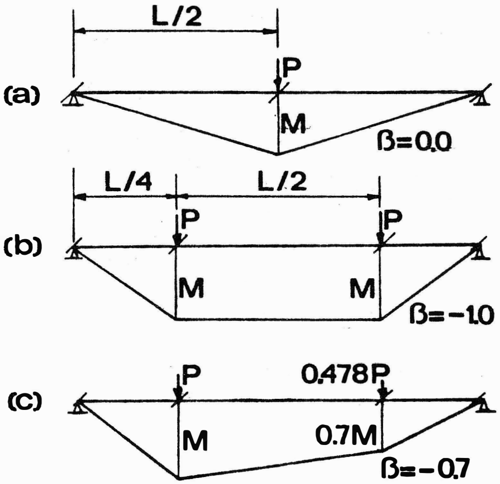

Expt. No.	L (m)
1	11.0
2	9.0
3	8.0
4	6.0
5	5.0
6	7.0
7	7.0
8	8.0
9	9.0

FIGURE 2: Test loading arrangements

Of the three loading patterns only that in Fig. 2(a) produces the equivalent of a simply supported beam under end moments. It has been noted (17) that simply supported boundary conditions for minor axis rotation and warping exist at the central braced point, hence each beam segment in Fig. 2(a) buckles independently of the other. It is difficult, however, to conceive of a convenient loading system guaranteeing simply supported end conditions and a general moment gradient. The arrangements in Figs. 2(b) and 2(c) result in critical central segments with restraining segments at the ends. As the response of a restrained segment only approximates that of a stockier simply suppoprted beam under the same moment gradient, it may well be that the theoretical curves in Fig. 1 will never receive precise checking by experimentation. Still, test beams loaded in the manner of Figs. 2(b) and 2(c) suffice for checking the influence of moment gradient. Quarter point loading was chosen over third point or other as considerable economies of material could be achieved while keeping point load magnitudes within reasonable limits.

2.3 Beam Type and Section Properties

The test beams were taken from six standard fifteen metre lengths of Universal Beam designated 250UB37.3. The beams were rolled by B.H.P., South Australia and were ordered from a single rolling batch. The particular size was chosen over others after detailed analyses in which were considered the handling of specimens, the available area of strong floor and the expected test load levels. Mean section dimensions and properties of each of the standard lengths are presented in Table 1. Flange widths and thicknesses and section depths were read at metre intervals. Web thicknesses were taken near sawn or flame cut ends. Fillet radii were measured wherever saw cutting provided an undistorted end section. Web-off-centre measurements were taken at random but were small (< 0.5 mm) and well within the allowable tolerance (18). The standard dimensions and properties (19) are also listed in Table 1. As well the table nominates the various test beams taken from each standard length. Test beam numbering is in Fig. 2.

TABLE 1

Section Dimensions and Properties

No.	Expt.* Nos.	mm							mm^2	$\times 10^6$ mm^4		$\times 10^3 mm^4$	$\times 10^{10}$ mm^6
		T_t	T_b	T_w	W_t	W_b	D	r	A	I_x	I_y	J	I_ω
1	6,7	10.49	10.83	6.78	147.72	147.49	256.31	7.5	4788	55.46	5.72	152.9	8.631
2	5,9	10.85	10.44	6.78	147.57	147.88	256.32	7.5	4787	55.45	5.73	152.6	8.642
3	4,3	10.65	10.53	6.58	147.78	148.28	256.14	7.5	4729	55.03	5.73	148.1	8.636
4	1	10.57	10.55	6.58	147.34	148.89	256.24	7.5	4734	55.14	5.73	147.4	8.642
5	8	10.78	10.44	6.78	147.61	147.83	256.28	7.5	4776	55.29	5.71	151.4	8.611
6	2	10.77	10.57	6.82	147.43	147.85	256.35	7.5	4801	55.58	5.73	153.3	8.648
Std.**	-	10.90	10.90	6.40	146.4	146.4	256.0	7.62	4750	55.60	5.71	155.0	8.576

* See Figure 2

** Reference 19

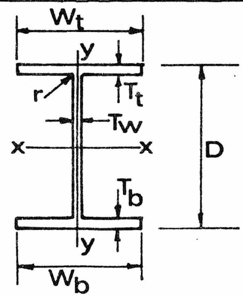

3. SUBSIDIARY TESTS

3.1 Yield Stress and Young's Modulus

A total of 25 tension coupons, 17 from flanges and eight from webs were tested to determine mean flange and web yield stresses. The rate of plastic straining was kept below .00002/sec. which is within the definition of a low straining rate (20). The purpose in adopting this was to match the rate likely to occur in the buckling experiments and hence to obtain representative yield stresses. With all coupons the lower yield stress varied during testing, fluctuations of one or two percent being recorded after first yield and before strain hardening. Average yield stresses have been found from minimum lower yield stresses, distributions of which are given in Fig. 3.

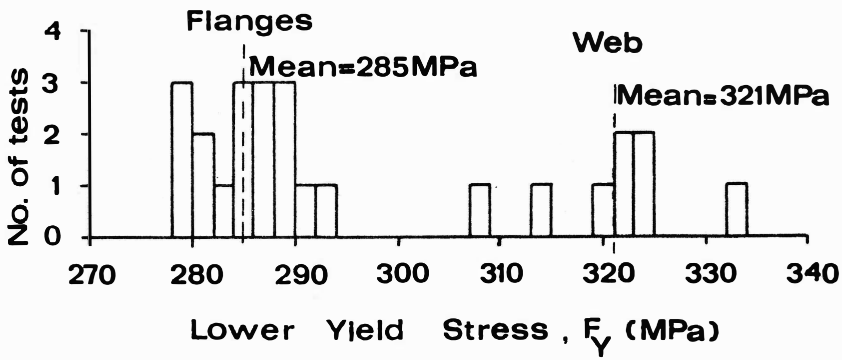

FIGURE 3: Tension test histograms

Values of Young's Modulus were obtained from 12 of the tests. The mean value is indicated in Fig. 4 and has been used in calculations.

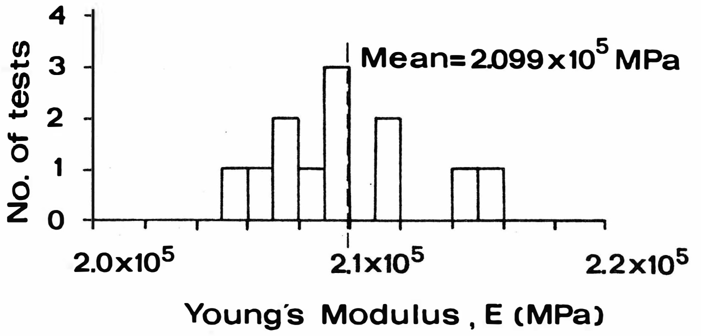

FIGURE 4: Young's Modulus

3.2 Residual Stresses

Six sets of residual strain measurements were taken, two from each of three standard lengths of beam. Double gauge lengths of 100 mm were located centrally in 1.8 metre offcuts . At each gauge length end 48 steel balls were punched into the positions shown in Fig. 5. A mechanical extensometer (Huggenberger Tensotast) was used to record gauge length changes accompanying the longitudinal sectioning of the 250 mm central portions containing the two gauge lengths. All cutting was by slow band-sawing.The longitudinal cut locations are marked in Fig. 5.

Residual strains were calculated as change in gauge length after longitudinal sectioning divided by original length in the 1.8 metre offcut. Four measurements, two of the gauge length and two of a standard bar for temperature compensation were required for each gauge length change. Each measurement was taken several times and, generally, a repeatability of between +/-.0005 mm and +/-.001 mm about the mean was achieved. As averages were used in strain calculations, an unfavourable combination of errors could give a cumulative length change error of +/-.002 mm to +/-.004 mm with a corresponding residual stress error of +/-4 MPa to +/-8 MPa.

Further sectioning was performed on one set of 250 mm slices. These were reduced in length to 150 mm with one gauge length retained but no significant change in ball separation was evident. Additional longitudinal slicing between the outermost flange gauge lengths also produced negligible changes in either gauge length. This particular sawing was left until last through concern that a fine flange tip slice might bow while being separated from the main body of the specimen. Finally, attempts were made to separate the flange and web gauge lengths in the slices containing the fillets (see Fig. 5). This induced considerable bowing in the web portions. The flange gauge lengths remained sensibly the same.

The residual stresses in Fig. 6 have been calculated using a Young's Modulus of 2.099×10^5 MPa and mean residual strains from matching pairs of gauge lengths on opposite sides of the flanges and webs. The results are reasonably consistent and so can be taken as representative of the residual strsses in all six standard beam lengths. The web stress patterns appear typically undisturbed (21) whereas the flange patterns show a considerable penetration of the effects of roller straightening. This was evident on all standard lengths where continuous yield line patterns extended well into the flanges.

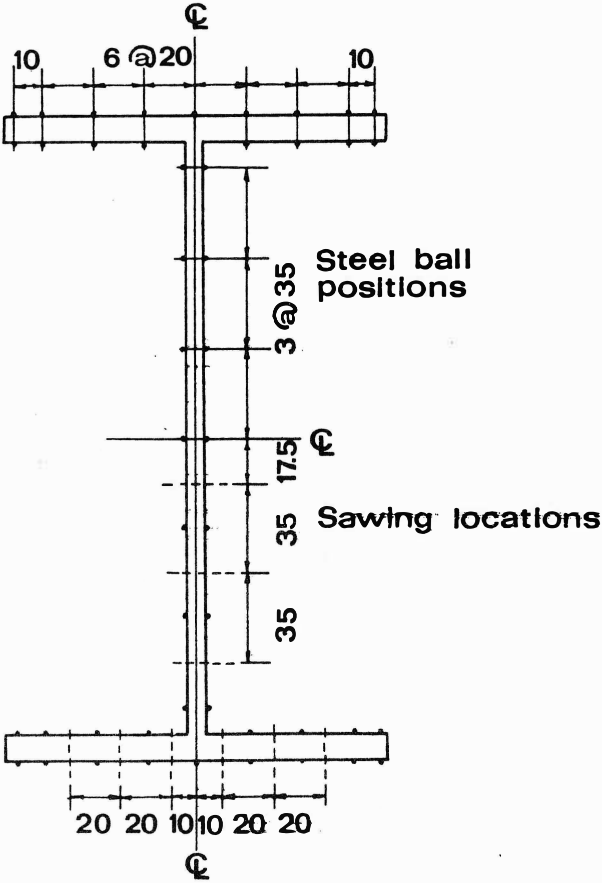

FIGURE 5: Steel ball positions and sawing locations

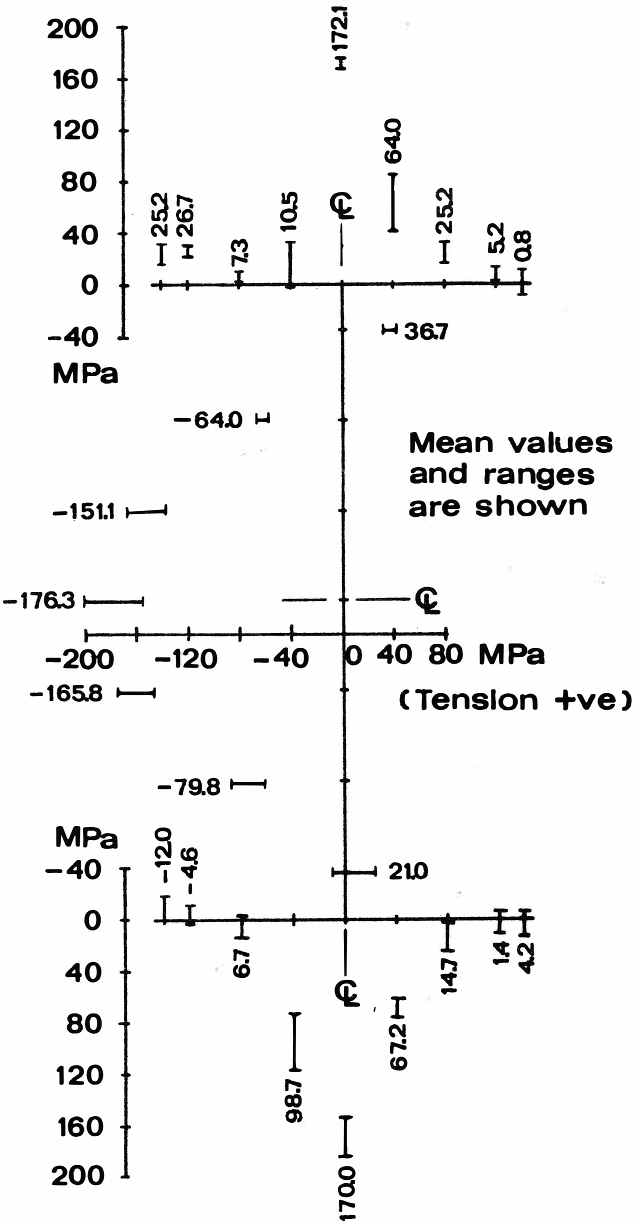

FIGURE 6: Residual stresses

3.3 Plastic Moment Tests

Two experiments were conducted to check values of plastic moment calculated with section dimensions from Table 1 and average flange and web lower yield stresses from Fig. 3. The specimens were tested in the manner shown in Fig. 7. Load was applied through a cylindrical loading head which acted also to restrain the top flange. A dial gauge was used to measure the central deflection. Load-deflection curves are given in Fig. 7.

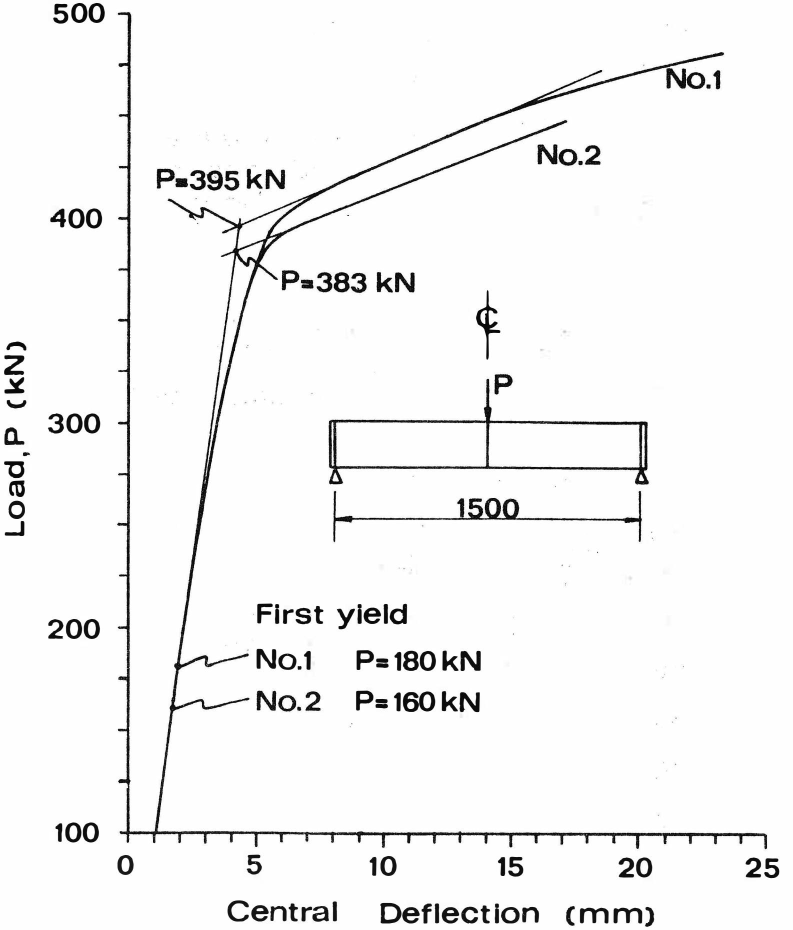

FIGURE 7 Load-deflection curves for plastic moment tests

Both curves have two distinct segments but no yield plateau. Baker, Horne and Heyman (22) discuss the features and disadvantages of single point load tests and conclude that results of tests with two point loads are more likely to agree with simple plastic theory. In Table 2, the test moments calculated from loads at the curve knees (see Fig. 7) are compared with predictions.

TABLE 2: Plastic moments

TEST No.	BEAM No.	PLASTIC MOMENT (kN.m) Calculated (22)	Experimental	LOAD (kN)
1	6	142.3	148.1	395
2	4	141.2	143.6	383

The moments for specimen 2 are in close agreement. A larger discrepancy occurs for specimen 1. A contributing factor is the varying strain rate at which the first experiment was conducted. As yielding commenced the rate of load-point deflection was allowed to increase five- and ten-fold over an initial value of around .02 mm/sec. Strain rates grossly exceeded that used in tension tests. With specimen 2, the same initial deflection rate was used but once yielding began the load was held constant until dial gauge movement had reduced to a rate of less than .02 mm/min. Load increases were applied in small increments and in a gradual manner so that the deflection rate did not exceed .02 mm/sec. The rates of plastic straining were thus maintained close to those used in the tension tests.

3.4 Stub Column Tests

As a further check on average section and material properties, one long (760 mm) and one short (300 mm) stub column specimens were prepared in the manner outlined in Ref. 23. The columns were loaded in a static manner. Axial strain rates conformed to the definition of a low rate plastic straining (20). Load-axial strain curves are given in Fig. 8 along with the theoretical squash load which agrees well with the experimental values.

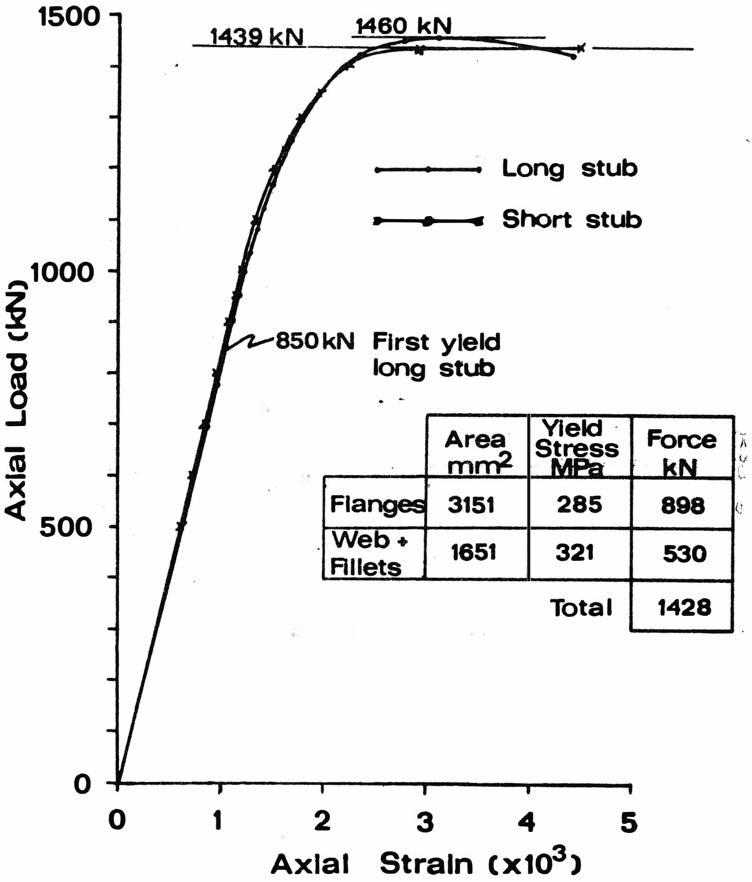

	Area mm^2	Yield Stress MPa	Force kN
Flanges	3151	285	898
Web + Fillets	1651	321	530
		Total	1428

FIGURE 8: Load-axial strain curves for stub column tests.

The longer specimen retained undisturbed residual stresses in the mid-height region (23). Its first yield coincided with a load of around 850 kN, the corresponding stress being 177 MPa. This implies that the peak residual compressive stress in the web was at least 144 MPa, a value which is at the lower end of the range of measured stresses (155 - 201 MPa). Such an estimate of residual stress is less reliable than those in Section 3.2.

4. APPARATUS

4.1 General Arrangement

The line diagram in Fig. 9 identifies the components of apparatus used to load, brace and support the test beams. The figure includes a simplification of the diagram in more conventional symbols. The various features of the sketches can be recognised in the accompanying photographs.

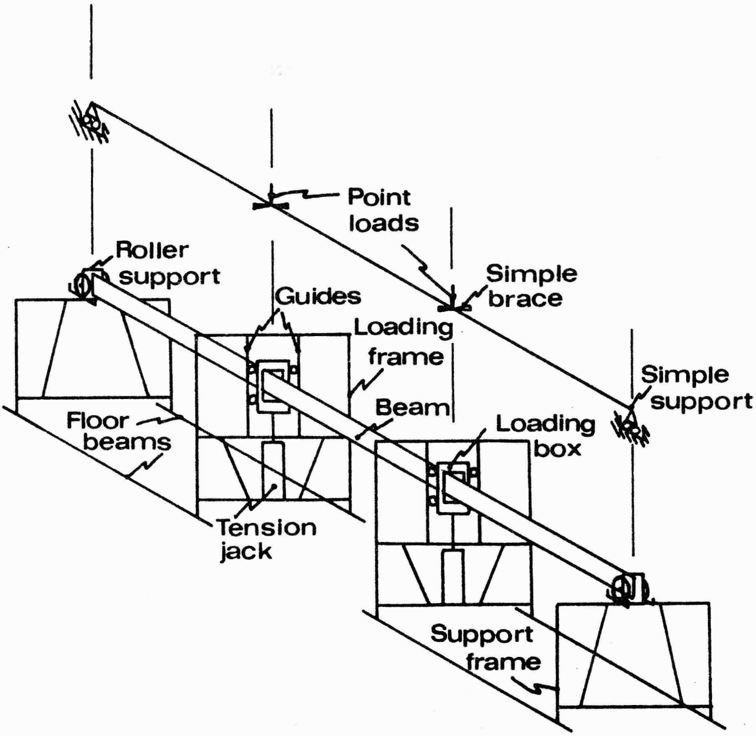

FIGURE 9: Line diagrams of apparatus

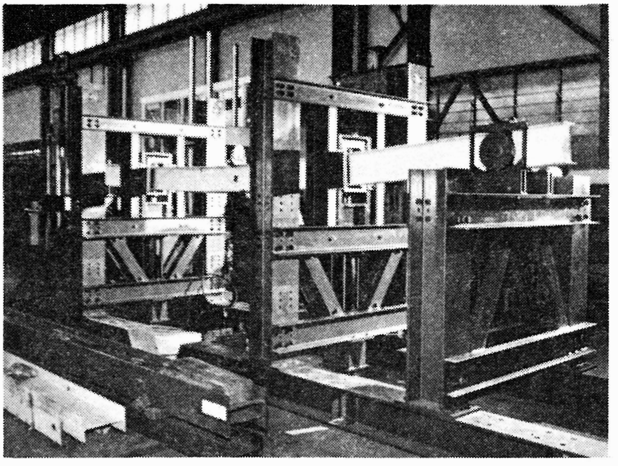

FIGURE 10: General arrangement of apparatus

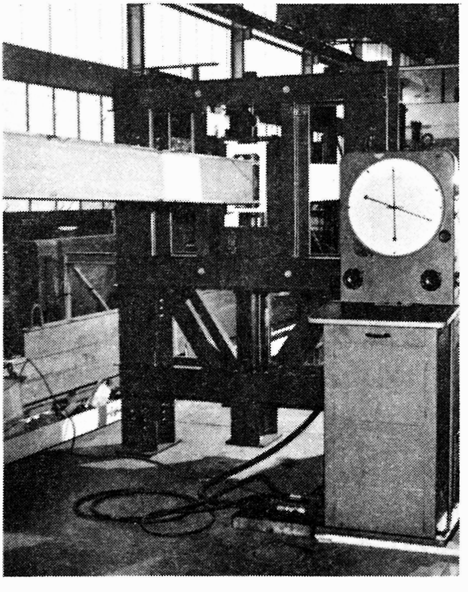

FIGURE 11: Loading frame

The general arrangement in Figs. 9 and 10 was typical of that used for tests with two point loads. The loading and support devices were mounted on loading and suport frames. These were connected to floor beams which in turn were bolted to a strong floor. Different segment lengths were set by altering the frame positions on the floor beams and, in some instances, by shifting the floor beams as well. For the central point load tests a single loading frame was bolted directly to the floor. This is shown in Fig. 11 which provides a closer view of a loading frame, guides, load box and hydraulic jack with its dynamometer in the foreground.

To prevent relative movement of the joined parts, all connections within the frames were either welded or made with friction grip bolts. The frames and floor beams require little description other than that provided by the various photographs. Other items will be discussed in more detail.

4.2 Roller Supports

Figure 10 shows a roller support to which a beam is bolted. An arrangement of bearings, rollers and guiding surfaces ensures that the cross-section at the connection is restrained from twisting and moving laterally whilst remaining free to warp, to move longitudinally and to rotate about the major and minor axes. The supports are described fully by Kitipornchai (1) and have been used more recently by Poowanachaikul and Trahair (24).

4.3 Loading Boxes

Figure 11 shows load being applied by a jack in tension reacting against the lower cross-beam of a loading frame. The jack ram is seen to connect to a loading box near the mid-height of the frame. More detail is provided in the cross-sectional view of Fig. 12.

The loading box comprises outer and inner boxes connected via pins welded to the inner box and mounted in bearings housed in the outer box. The bearings are able to accept both radial and axial load. Relative to the outer box the inner one is free to rotate about the axis of the bearings which closely approximates the elastic major axis of the test beams when in place.

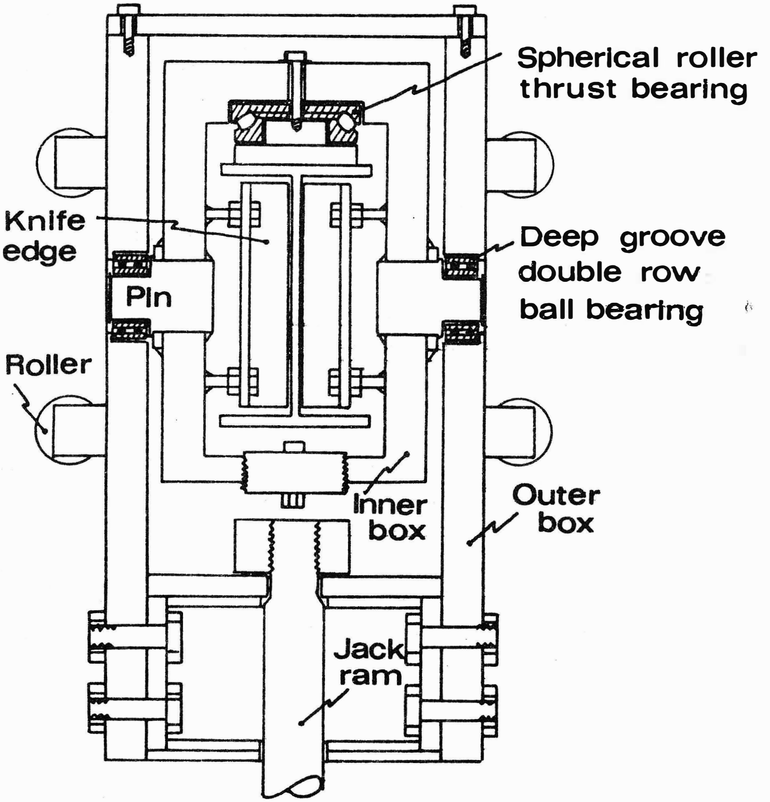

FIGURE 12: Cross-sectional view of loading box

Within the inner box are two adjustable knife edges which prevent the beam cross-section at the load point from moving laterally and from twisting relative to the inner box. A spherical roller thrust bearing with axial and radial load capacities is housed in the top plate of the inner box. The beam is loaded at top flange level through this bearing which permits minor axis rotation under load.

The outer box has eight rollers, four on each side to bear against vertical machined guide surfaces bolted to the loading frame. Small clearances (< 0.2 mm) were provided to prevent jamming. The vertical loading inhibits any rotation of the outer box in the plane of the test beam web save the small amount accompanying axial shortening of the central segment during quarter-point loading tests. The jack base-to-frame connection permits free rotation of the jack in this plane. Preliminary analysis indicated that the axial load caused by this tilting of the jacks would not exceed 0.2 kN, a negligible amount.

To summarise, the load path is from the jack to the outer box then through the thrust bearing to the beam. The apparatus provides a simple brace preventing lateral movement and twisting. It was chosen over the more common fixed knife edge arrangement to avoid the undesirable friction sometimes reported (9). Comparisons of measured and theoretical vertical deflections in Fig. 13 show that the loading boxes performed satisfactorily. Figure 14 shows a buckled beam with considerable minor axis rotation at the central load point.

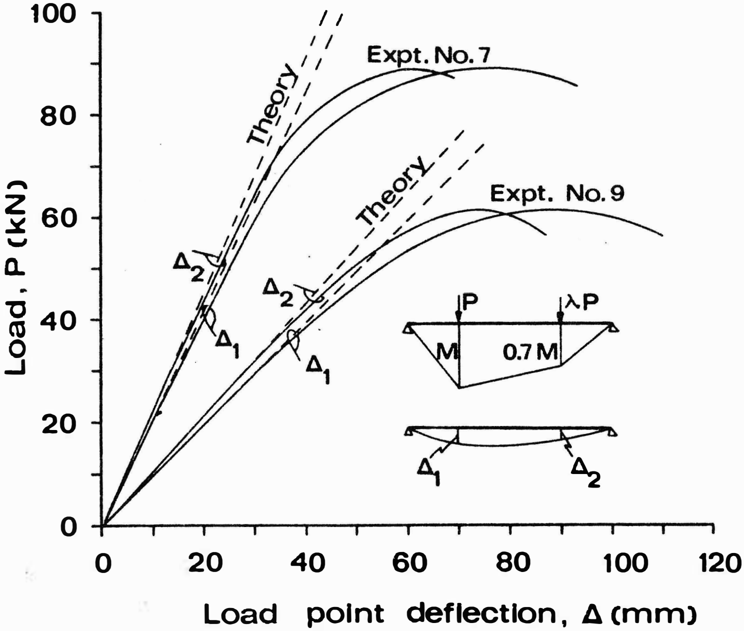

FIGURE 13: Load point deflections

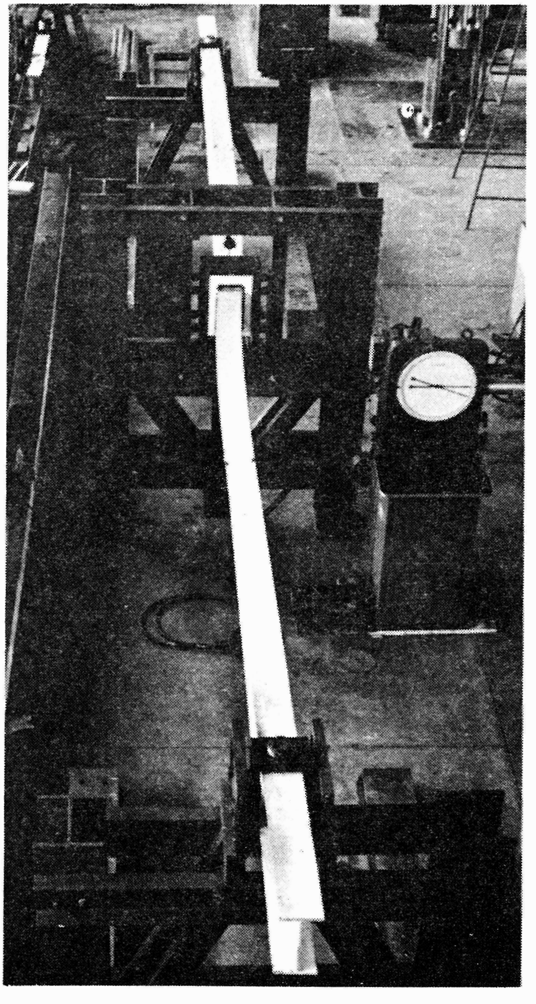

FIGURE 14:Buckled beam with mid-point load

4.4 Hydraulic Jacks

Test loads were applied by Parker Hannifan hydraulic jacks with the piston rods or rams in tension. For the $\beta = 0.0$ and $\beta = -1.0$ series, a single dynamometer was used. A separate dynamometer for each jack provided the unequal quarter-point loads in the $\beta = -0.7$ experiments.

Before the tests began, both jacks were calibrated with each dynamometer against an Amsler universal testing machine which itself is regularly calibrated to Grade A specifications (25). The process was repeated after the final experiment. Each calibration involved several tests with the jack ram in different starting positions. Small ranges of the ram stroke were covered in each instance to disclose any variation in jack performance.

The consistency of response during the first calibrations led to the adoption of calibration curves for load measuring purposes as opposed to the incorporation of load cells or other devices into the apparatus. The results of the second calibrations support well those of the first despite some small changes in performance. All calibration results were used to determine average response curves for each jack. Individual calibration figures differ from the mean by at most +/-0.7% at any nominal load level in excess of around 50% of the beam failure loads. Small surcharges compensated for the differences in response when both jacks were driven by a common dynamometer.

The mean results of all calibrations are given in Fig. 15 along with typical calibration figures. The positions of fully extended (out) and one half withdrawn (1/2 out) correspond approximately to the extremes of ram position occurring during the buckling experiments.

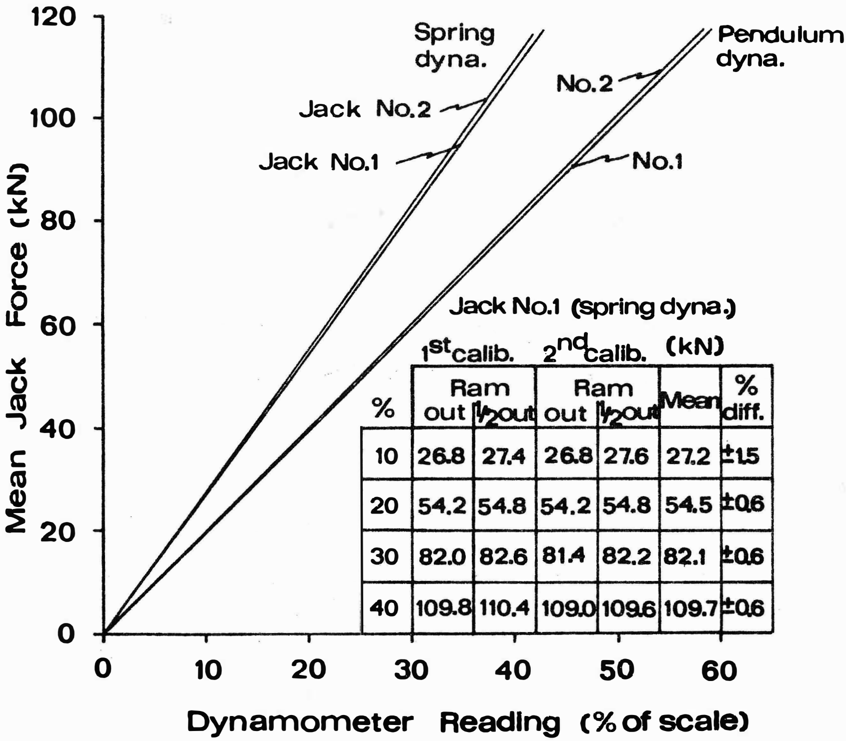

%	1st calib. Ram out	1st calib. Ram ½ out	2nd calib. Ram out	2nd calib. Ram ½ out	Mean (kN)	% diff.
10	26.8	27.4	26.8	27.6	27.2	±1.5
20	54.2	54.8	54.2	54.8	54.5	±0.6
30	82.0	82.6	81.4	82.2	82.1	±0.6
40	109.8	110.4	109.0	109.6	109.7	±0.6

FIGURE 15: Calibration curves for hydraulic jacks

During tests with two dynamometers, loads near the failure load were controllable to +/-0.25 kN according to the fluctuations accompanying progressive yielding and deformation of the beams. A single jack or a pair driven by the one dynamometer gave more stable loads. Actual critical segment moment gradients have been estimated from mean calibration figures and are given in Table 4. They vary from the intended values by +/-0.06%.

4.5 Instrumentation

A test beam with typical instrumentation is shown in Fig. 16.

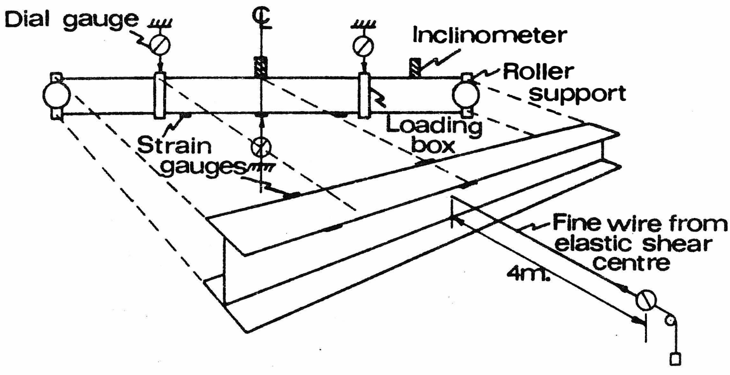

FIGURE 16: Test beam instrumentation

The measurements of deflection and strain provide a load-deformation history for each beam. However, some were of more immediate use. For example, measurements of strain, lateral deflection and twist were used in monitoring the state of the test beam. These indicated the growth of buckling deformations and the tendency or otherwise of the inelastic beam to stabilise in a deformed position under constant load. Particularly useful in identifying the onset of instability were the strain readings from compression flange tip gauges. These values were plotted as the experiment progressed. Radical strain changes became obvious as one of each pair of tip gauges was placed in tension by the lateral bowing associated with the development of the buckled shape. This and other information helped in determining the size and rate of application of load increments and, as well, the time between the application of the increments. Figure 17 shows compression flange strains from Expt. 7.

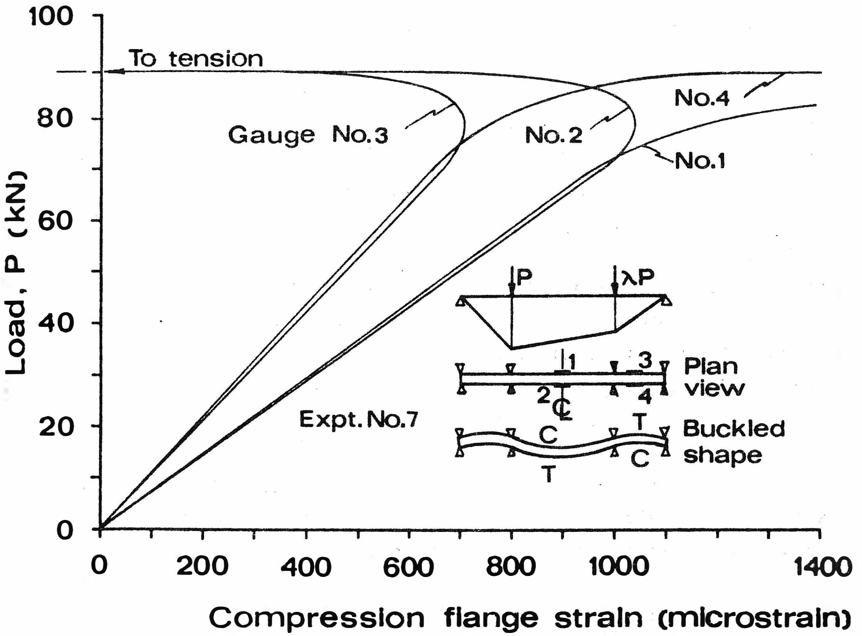

FIGURE 17:Flange tip strain variations

Measurements of vertical displacement and elastic strains were used in checking that the correct moment gradients had been established and that load magnitudes had been as assumed. Attempts to record accurately the first yield at the centre of the tension flange through a strain rate change and thus to verify measured residual stresses were generally unsuccessful. The peaked distribution of flange residual stress (see Fig. 6) led to the yielded material being restrained by elastic material in close proximity so that early strain rate changes could be ascribed as easily to gauge drift.

5. BUCKLING EXPERIMENTS

5.1 Beam Preparation and Measurement of Geometrical Imperfections

The test beams were arranged in the apparatus described with webs vertical at the load and support points. This was achieved in part by the earlier adjustment of the loading box knife edges to locate the webs cetrally and parallel to the inner box walls. As well, the loading frames were aligned with corresponding pairs of vertical guide surfaces coplanar. Webs at the end cross-sections were made vertical by the levelling of the end roller support guides (see Fig. 10). The final positioning of the roller support guides was made after the beam had adopted its own resting place. The guides were not preset so as to avoid the possible imposition of a minor axis bending moment pattern on the test beam. It eventuated that all but three of the beams lay practically straight. When the beams and apparatus were satisfactorily arranged geometrical imperfections were measured.

Initial lateral bow at the elastic shear centre and initial twist within the beam segments have been calculated using measurements of flange tip deviations from fine lines streteched between the beam ends. Differences between upper and lower flange outstands were taken into account. The maxima which occurred generally near mid-segment are given in Table 3.

TABLE 3: Geometrical imperfections

No.	β	L (m)	Segment Maxima: Bow/seg. length 1	2	3	Twist (rad.) 1	2	3	Beam bow / Beam length
1	0.0	11.0	-.0002	.0002	-	.003	.002	-	.0001
2	0.0	9.0	.0003	.0004	-	<.001	-.002	-	.0002
3	0.0	8.0	.0002	.0003	-	-.003	.003	-	.00025
4	-1.0	6.0	-.0008	.0004	-.0003	<.001	.003	<.001	.0003
5	-1.0	5.0	.0004	.0005	.0004	<.001	.001	<.001	.0003
6	-1.0	7.0	0.0	.0007	-.0003	<.001	.003	<.001	.0008
7	-0.7	7.0	0.0	.0004	0.0	<.001	-.002	<.001	.0005
8	-0.7	8.0	-.0005	.0003	-.0005	<.001	-.002	<.001	.0004
9	-0.7	9.0	.0002	.0004	.0002	<.001	.003	<.001	.0007

Signs indicate the relative directions of segment lateral bow within each beam. Positive twists combine with the corresponding lateral bows to worsen the imperfections. The extreme right hand column in Table 3 gives the maximum overall bow from a straight line joining the end section shear centres.

The imperfections are greater than those reported by Fukumoto, Itoh and Kubo (16). The mean non-dimensionalised initial bow (bow/length) of 75 beams in that reference was 0.00008 compared with a mean of 0.0003 in Table 3. Both figures are much less than the commonly used 0.001. The mean initial rotation from Ref. 16 is .0013 radians while values from Table 3 for the longer segments have an average of .0023 radians. In Ref. 26 larger initial twists are reported for simply supported beams with spans similar to the longer segment lengths of the present series.

5.2 Testing Procedure

The experiments began with a trial loading in the elastic range to seat the jacks and to check the functioning of the instruments and apparatus. The test load was then applied in increments, the size and rate of application of which depended on the proximity to failure estimated from the development of inelasticity and the growth of buckling deformations. Increments were generally as large as 10 kN in the early stages of testing and as small as 0.5 kN near buckling. Application rates reduced from around 5 kN/min to 0.5 kN/min as the experiment proceeded. For the $\beta = -0.7$ tests with two dynamometers, load scales were arranged to indicate identical loads when true loads were at the desired ratio. This enabled the correct load ratio to be maintained during the application of load increments.

Each load was held until dial and strain gauge readings indicated that the beam had settled. Some higher loads were held for over 15 mins. while the rates of increase of in-plane and out-of-plane movement gradually reduced. The attainment of maximum load was followed by load shedding and the development of gross deformations. Attempts to maintain the maximum load were unsuccessful. All beams exhibited a rapid loss of strength.

5.3 Test Results

The results of the experiments are presented in Table 4. Beam self weight has not been included in either the test figures or in the predictions of elastic and inelastic capacities. The elastic buckling moments in Table 4 have been found by Finite Integral analysis (2) using 18 divisions along the beams and the true moment gradients rather than the nominal ones. Use of the nominal moment gradients causes only slight changes to the values in the table.

TABLE 4: Test Results

Expt. No.	Description	β	Load P (kN)	M_E (kN.m)	M_p (kN.m)	$\sqrt{M_p/M_E}$	M_c/M_p
1		0.0	47.1	153.3	141.2	.960	.917
2	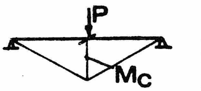	0.0	62.6	205.2	142.3	.833	.990
3		0.0	71.0	241.4	140.6	.763	1.010
4		-.996	89.8	413.0	140.6	.583	.958
5	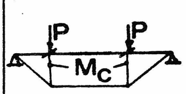	-.996	107.7	572.7	141.9	.498	.949
6		-.996	71.6	315.3	141.9	.671	.883
7		-.703	92.8	366.3	141.9	.622	.996
8	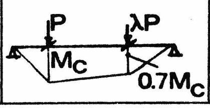	-.696	78.2	292.5	141.5	.696	.960
9		-.696	67.2	242.6	141.9	.765	.925

The test points are plotted in Fig. 18. Also in the figure are test results from Ref. 9, theoretical curves for simply supported beams under moment gradients (12) and the Australian design curve (4) calculated by assuming a load factor of 1.67 and a shape factor of 1.10.

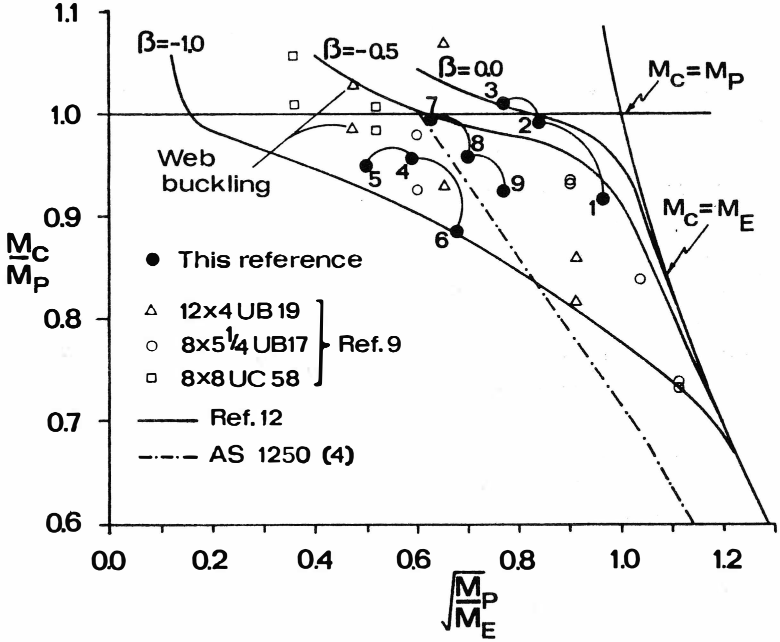

FIGURE 18: Test results and capacity curves

The results of the current series are grouped clearly according to moment gradient. The variation in capacity between groups is significant and this supports a multiple capacity curve approach to design such as that developed in Ref. 12. The spread of results demonstrates the inadequacy of a single design curve of the type in Fig. 18. Some test points are well above the line and some are well below. Slendernesses for the attainment of the fully plastic moment are not predicted with accuracy. In fairness, the single curve from Ref. 4 was not intended to provide a lower bound but rather something of a mean value line to the results of earlier experiments (see Fig. 1). However, the discrepancies between the design curve and, for example, the $\beta = 0.0$ test points are significant.

In general, the results support theoretical trends concerning the influence of moment gradient. It has been noted in Section 2.2 that the $\beta = 0.0$ test arrangement produced the equivalent of a simply-supported beam with a single end moment. Two of the test results (Expts. 2 and 3) agree very closely with predictions. Although the imperfections of the theoretical beam involved only residual stress, it appears that the high levels assumed (see Ref. 12 and Fig. 1) have adequately represented the combined effect of smaller residual stresses and geometrical imperfections in the real beams. One result (Expt. 1) falls below the $\beta = 0.0$ curve. It does so in a region of slenderness where theory predicts that yielding has only a marginal influence on the buckling load. The test result implies that geometrical imperfections may be of more consequence than residual stresses for beams in this slenderness region.

The uniform moment results fall close to the theoretical curve, allowing that the test arrangement did not produce the precise equivalent of a simply supported beam with end moments. Figure 18 does not include a theoretical curve for $\beta = -0.7$. However, the test points lie as anticipated in a group between the other two sets.

The experiments of Dibley (9) have much in common with the uniform moment tests as they involved beam and column sections with two equal loads either at the quarter points or at points closer to the end supports. The current test results fall at the lower boundary of the group from Ref. 9. The $\beta = -0.7$ test results lie above the mean curve of this group. Part of the difference between the uniform moment results may be due to the loading rates adopted.

In Section 5.2 an essentially static loading procedure is described. Records of load, time and strain show that a higher loads (> 0.9 of the buckling load) the rate of application of load increments did not exceed 0.5 to 1.0 kN/min. This had the effect of limiting the maximum strain rate at the centre of the tension flange to around a few microstrain per second. This rate is generally less than that used in tension tests described in Section 3.1 where an upper limit of 20 microstrain/sec. was adopted. It was felt justifiable to allow the strain rate to fall as, while the tension test results would remain valid, the lower rate of straining would permit a gradual and full distribution of yielding to take place within the test beams. The feel of the experiments was that higher loads could have been attained had a faster loading rate been adopted. The tests in Ref. 9 were conducted at a constant strain rate of around 40 microstrain/sec., identical to that used in associated tension tests. The higher rate of loading may have led to maximum loads in excess of static loading capacities.

Another factor which might contribute to the difference involves adjustments made to test results in Ref. 9. Test loads have been modified to remove the component of friction between test beams and loading apparatus. Corrections of up to 16.9% of the registered failure load were estimated from differences between measured and theoretical deflections while test beams were in the elastic range. Whether or not allowance was made for likely increases in friction during the growth of out-of-plane deformations at later stages of the tests is not clear. Whatever was done, load adjustments of this type are approximate and undesirable.

6.0 CONCLUSIONS

Nine experiments comprising three groups of three have been conducted to investigate the influence of major axis moment gradient on the capacity of inelastic beams. Three moment patterns were selected ranging from uniform bending to the equivalent of a single end moment. Within each group of three experiments, beam slendernesses were chosen such that buckling should occur in the loading range between first yielding and the attainment of the plastic moment. This was achieved for all but one beam.

The results demonstrate that capacity is a function of moment gradient. Beams with the less severe gradients were able to sustain higher moments than could much stockier beams in uniform bending. This became more pronounced as loading conditions eased. Furthermore, each set of three results formed a distinct group. Theory predicted closely the position of one such group on a non-dimensional plot of capacity versus slenderness. A comparison of the other groups with theoretical results not so directly applicable shows that real beam behaviour follows predicted trends.

These findings support recent attempts to introduce design methods with multiple beam capacity curves based on moment gradient (12). A comparison of the results with the design provisions of the Australian code (4) shows that a typical single design curve is not adequate.

7.0 ACKNOWLEDGEMENTS

The authors wish to acknowledge the extensive participation of laboratory staff. In particular, they wish to thank Messrs. R. Eaton, D. Foote, and L. Abrahamson. The authors are indebted also to Mr. R. Nilsson of the academic staff for developing a strain recording and plotting system.

APPENDIX A - NOMENCLATURE

Symbol	Meaning
A	Cross-section area
E	Young's modulus of elasticity
F_Y	Yield stress
I_x	Major axis second moment of area
I_y	Minor axis second moment of area
I_ω	Warping section constant
J	St. Venant torsion constant
L	Beam length
M	Major axis moment
M_c	Buckling moment
M_E	Elastic buckling moment
M_p	Plastic moment
P	Point load
β	Ratio of major axis end moments
λ	Factor

APPENDIX B - REFERENCES

1. KITIPORNCHAI, S., "Stability of Steel Structures", Ph.D. Thesis, University of Sydney, 1973.

2. RICHTER, N.J., "Application of the Finite Integral Method to Lateral Buckling of Beams", M.Eng.Sc. Thesis, University of Queensland, 1979.

3. TRAHAIR, N.S., "Elastic Stability of Continuous Beams", J. Struct. Divn., ASCE, Vol. 95, No. ST6, Proc. Paper 6632, June 1969, pp. 1295-1312.

4. STANDARDS ASSOCIATION OF AUSTRALIA, "AS 1250-1981 SAA Steel Structures Code", SAA, Sydney, 1981.

5. AMERICAN INSTITUTE OF STEEL CONSTRUCTION, "Specification for the Design, Fabrication and Erection of Structural Steel for Buildings", AISC, New York, 1969.

6. BRITISH STANDARDS INSTITUTION, "BS 449:1969 Specification for the Use of Structural Steel in Buildings", BSI, London, 1969.

7. FUKUMOTO, Y. and KUBO, M., "An Experimental Review of Lateral Buckling of of Beams and Girders", Proceedings of the International Colloquium on Stability of Structures Under Static and Dynamic Loads", SSRC - ASCE, Washington D.C., March 1977, pp. 541-562.

8. KITIPORNCHAI, S. and TRAHAIR, N.S., "Inelastic Buckling of Simply Supported Steel I-Beams", J. Struct. Divn., ASCE, Vol. 101, No. ST7, Proc. Paper 11419, July 1975, pp. 1333-1347.

9. DIBLEY, J.E., "Lateral Torsional Buckling of I-Sections in Grade 55 Steel", Proceedings, I.C.E., Vol. 43, August 1969, pp. 559-627.

10. GALAMBOS, T.V., "Laterally Unsupported Beams", ECCS, Introductory Report, Second International Colloquium on Stability, Tokyo, Liege, Washington (1976, 1977) pp. 365-373.

11. VINNAKOTA, S., "Inelastic Stability of Unsupported I-beams", Second National Symposium on Computerised Structural Analysis and Design,

School of Engineering and Applied Science, George Washington University, Washington D.C., March 1976.

12. NETHERCOT, D.A. and TRAHAIR, N.S. "Inelastic Lateral Buckling of Determinate Beams", J. Struct. Divn., ASCE, Vol. 102, No. ST4, Proc. Paper 12020, April 1976, pp. 701-717.

13. KITIPORNCHAI, S. and DUX, P.F., discussion of "Inelastic Lateral Buckling of Determinate Beams" by D.A.Nethercot and N.S. Trahair, J. Struct. Divn., ASCE, Vol. 103, No. ST2, February 1977, pp.461-462.

14. DUX, P.F. and KITIPORNCHAI, S., "Approximate Inelastic Buckling Moments for Determinate I-Beams", Civil Engng Trans., Institution of Engineers, Australia, Vol. CE20, No. 2, 1978, pp. 128-133.

15. LINDNER, J. et al., "Laterally Supported and Unsupported Beams", ECCS, Introductory Report, Second International Colloquium on Stability, Tokyo, Liege, Washington (1976, 1977), pp. 127-143.

16. FUKUMOTO, K., ITOH, V. and KUBO, M., "Strength Variation of Laterally Unsupported Beams", J. Struct. Divn., ASCE, Vol. 106, No. ST1, Proc. Paper 15142, January 1980, pp. 165-181.

17. DUX, P.F. and KITIPORNCHAI, S., "Buckling Approximations for Laterally Continuous Elastic I-Beams", Univ. of Qld., Dept of Civil Engg., Research Report No. CE11, April 1980.

18. "BHP-AIS Hot Rolled Carbon Steel Sections and Plates", Broken Hill Proprietary Co. Ltd, and Australian Iron and Steel Pty Ltd, 1969.

19. "B.H.P. Rolled Sections and Plates - Abridged Edition", Broken Hill Proprietary Co. Ltd, 1974.

20. STANDARDS ASSOCIATION OF AUSTRALIA, "AS 1391-1974 Methods for Tensile Testing of Metals", SAA, Sydney, 1974.

21. YOUNG, B.W., "Residual Stresses in Hot Rolled Sections", Joint Colloquium on Column Strength IABSE - CRC - ECCS, Paris, November 1972.

22. BAKER, J.F., HORNE, M.R. and HEYMAN, J., "The Steel Skeleton", Vol. 2,

Plastic Behaviour and Design, Cambridge University Press, 1956.

23. Column Research Council, "Guide to Design Criteria for Metal Compresion Members", Ed. B.G. Johnston, 2nd Edition, John Wiley and Sons, 1966.

24. POOWANNACHAIKUL, T. and TRAHAIR, N.S., "Inelastic Buckling of Continuous Steel I-beams", Res. Report R51, Dept Civ. and Str. Engg, Univ. of Shefield, November 1974.

25. STANDARDS ASSOCIATION OF AUSTRALIA, " AS 2193-1978 Methods for the calibration and grading of Force-Measuring Systems of Testing Machines", SAA, Sydney, 1978.

26. HECHTMAN, R.A, HATTRUP, J.S., STYER, E.F., and TIEDEMANN, J.L., "Lateral buckling of Rolled Steel Beams", Proceedings, ASCE, Engg. Mechs. Div., Vol 81, Separates, Proc.Pap. 797, September 1955.

CIVIL ENGINEERING RESEARCH REPORTS

CE No.	Title	Author(s)	Date
8	An Appraisal of the Ontario Equivalent Base Length	O'CONNOR, C.	February, 1980
9	Shape Effects on Resistance to Flow in Smooth Rectangular Channels	KAZEMIPOUR, A.K. & APELT, C.J.	April, 1980
10	The Analysis of Thermal Stress Involving Non-Linear Material Behaviour	BEER, G. & MEEK, J.L.	April, 1980
11	Buckling Approximations for Laterally Continuous Elastic I-Beams	DUX, P.F. & KITIPORNCHAI, S.	April, 1980
12	A Second Generation Frontal Solution Program	BEER, G.	May, 1980
13	Combined Stiffness for Beam and Column Braces	O'CONNOR, C.	May, 1980
14	Beaches:- Profiles, Processes and Permeability	GOURLAY, M.R.	June, 1980
15	Buckling of Plates and Shells Using Sub-Space Iteration	MEEK, J.L. & TRANBERG, W.F.C.	July, 1980
16	The Solution of Forced Vibration Problems by the Finite Integral Method	SWANNELL, P.	August, 1980
17	Numerical Solution of a Special Seepage Infiltration Problem	ISAACS, L.T.	September, 1980
18	Shape Effects on Resistance to Flow in Smooth Semi-circular Channels	KAZEMIPOUR, A.K. & APELT, C.J.	November, 1980
19	The Design of Single Angle Struts	WOOLCOCK, S.T. & KITIPORNCHAI, S.	December, 1980
20	Consolidation of Axi-symmetric Bodies Subjected to Non Axi-symmetric Loading	CARTER, J.P. & BOOKER, J.R.	January, 1981
21	Truck Suspension Models	KUNJAMBOO, K.K.@F. O'CONNOR, C.	February, 1981
22	Elastic Consolidation Around a Deep Circular Tunnel	CARTER, J.P. & BOOKER, J.R.	March, 1981
23	An Experimental Study of Blockage Effects on Some Bluff Profiles	WEST, G.S.	April, 1981
24	Inelastic Beam Buckling Experiments	DUX, P.F. & KITIPORNCHAI, S.	May, 1981

CURRENT CIVIL ENGINEERING BULLETINS

4 *Brittle Fracture of Steel — Performance of ND1B and SAA A1 structural steels: C. O'Connor (1964)*

5 *Buckling in Steel Structures — 1. The use of a characteristic imperfect shape and its application to the buckling of an isolated column: C. O'Connor (1965)*

6 *Buckling in Steel Structures — 2. The use of a characteristic imperfect shape in the design of determinate plane trusses against buckling in their plane: C. O'Connor (1965)*

7 *Wave Generated Currents — Some observations made in fixed bed hydraulic models: M.R. Gourlay (1965)*

8 *Brittle Fracture of Steel — 2. Theoretical stress distributions in a partially yielded, non-uniform, polycrystalline material: C. O'Connor (1966)*

9 *Analysis by Computer — Programmes for frame and grid structures: J.L. Meek (1967)*

10 *Force Analysis of Fixed Support Rigid Frames: J.L. Meek and R. Owen (1968)*

11 *Analysis by Computer — Axisymmetric solution of elasto-plastic problems by finite element methods: J.L. Meek and G. Carey (1969)*

12 *Ground Water Hydrology: J.R. Watkins (1969)*

13 *Land use prediction in transportation planning: S. Golding and K.B. Davidson (1969)*

14 *Finite Element Methods — Two dimensional seepage with a free surface: L.T. Isaacs (1971)*

15 *Transportation Gravity Models: A.T.C. Philbrick (1971)*

16 *Wave Climate at Moffat Beach: M.R. Gourlay (1973)*

17. *Quantitative Evaluation of Traffic Assignment Methods: C. Lucas and K.B. Davidson (1974)*

18 *Planning and Evaluation of a High Speed Brisbane-Gold Coast Rail Link: K.B. Davidson, et al. (1974)*

19 *Brisbane Airport Development Floodway Studies: C.J. Apelt (1977)*

20 *Numbers of Engineering Graduates in Queensland: C. O'Connor (1977)*